KEK/J-PARC-PAC 2012-9

Proposal for the J-PARC 50-GeV Proton Synchrotron
Revised in July, 2012

Spectroscopic study of hyperon resonances below $\bar{K}N$ threshold via the (K^-,n) reaction on Deuteron

S. Ajimura, S. Enomoto, K. Inoue, S. Kawasaki, H. Noumi (*Spokesperson/Contact Person), K. Shirotori
Research Center for Nuclear Physics (RCNP), Osaka University, Japan

K. Itahashi, M. Iwasaki, Y. Ma, H. Ohnishi, S. Okada, H. Outa, F. Sakuma, D. Tomono, K. Tsukada, T. Yamazaki
RIKEN Nishina Center, RIKEN, Japan

H. Fujioka, T. Hiraiwa, Y. Ishiguro, T. Nagae, Y. Sada
Kyoto University, Japan

M. iio, S. Ishimoto, M. Iwai, M. Sekimoto, S. Suzuki, A. Toyoda
High Energy Accelerator Research Organization (KEK), Japan

L. Busso, D. Faso, O. Morra
INFN Sez. di Torino, Italy

M. Bragadireanu, C. Curceanu, C. Guaraldo, M. Iliescu, L. Poli Lener, A. Romero Vidal, D. Sirghi, F. Sirghi, H. Tatsuno, O. Vazquez Doce
Laboratori Nazionali di Frascati dell'INFN, Italy

T. Fukuda, Y. Mizoi
Osaka Electro-Communication University, Japan

N. Ishibashi, A. Sakaguchi, K. Yoshida
Osaka University, Japan

P. Büehler, M. Cargnelli, T. Ishiwatari, J. Marton, E. Widmann, J. Zmeskal
Stefan Meyer Institute for Subatomic Physics, Austria

H. Bhang, S. Choi, H. Yim
Seoul National University, South Korea

H. Kou, M. Tokuda
Tokyo Institute of Technology, Japan

K. Tsukada
Tohoku University, Japan

P. Kienle
Technische Universiät München, Germany

L. Busso
Università di Torino, Italy

Y. Fujiwara, R. S. Hayano, T. Ishikawa, Y. Matsuda, M. Sato, T. Suzuki, H. Tatsuno
University of Tokyo, Japan

G. Beer
University of Victoria, Canada

(The collaboration members shown above have been updated since May, 2012.)

Proposal for the J-PARC 50-GeV Proton Synchrotron
Revised in July, 2012

Abstract:

We propose spectroscopic study of Λ(1405) via the (K^-,n) reaction on deuteron. This reaction is expected to enhance a virtual $\bar{K}N$ scattering, forming the Λ(1405) state. This reaction is a suitable channel to test $\bar{K}N$ coupling to Λ(1405). This subject is closely related to so-called two pole structure of Λ(1405) suggested by the chiral unitary model, which affects recent discussion on deeply bound kaonic nuclear states. The primary goal of the present study is exclusively to show the position and the width (for the line shape information) of the Λ(1405) resonance produced in the $\bar{K}N \rightarrow \pi\Sigma$ channel.

Summary of the proposed experiment:

Beam line : K1.8BR

Primary beam : 30 GeV, 0.9 μA (27 kW) proton

Secondary beam : 1.0 GeV/c K^-

Beam intensity : 2.0×10^5 per pulse (6 s spill interval)

Reaction : d(K^-,n)

Detectors : Backward decaying particle counters in addition to the E15 setup

Target : Liquid Deuterium, 8cm(1.352 g/cm^2)

Beam time : 120 shifts

Estimated Yield :

~19200 Λ(1405) $\rightarrow \Sigma^-\pi^+$ decay events

~4800 Λ(1405) $\rightarrow \Sigma^+\pi^-$ decay events

~350 Λ(1405) $\rightarrow \Sigma^0\pi^0$ decay events

1. Introduction

Quark configuration in a hadron is interesting since quark-quark or quark-antiquark correlations in a hadron will provide information to understand the mechanism of forming hadrons from quarks based on QCD. Particularly, hadrons including eccentric quark configuration and/or correlations carry important information, which are reflected in the property of the hadrons (mass, width, spin, isospin, parity, electromagnetic moments, etc) and formation of the hadrons as well as their decays.

Structure of $\Lambda(1405)$ is still unclear if it is a three-quark state or a meson-baryon molecular state or other exotic state. Many experimental attempts and theoretical analysis to reveal $\Lambda(1405)$ have been done, a part of which are briefly described in Appendix A. The review of particle physics [1] adopted the mass and width of the $\Lambda(1405)$ state obtained by analyzing the invariant mass spectrum of $\Lambda(1405)$ in the final $\pi^-\Sigma^+$ state via the 4.2 GeV/c K^- induced reaction on hydrogen [2,3]. The $K^-p \rightarrow \pi^0\pi^0\Sigma^0$ reaction was measured at BNL [4]. The final $\pi^0\Sigma^0$ state guaranteed the I=0 state of the parent particle. Theoretical analysis based on a chiral unitary model reproduced the measured invariant mass of $\pi^0\Sigma^0$ and claimed the evidence of the two-pole structure of $\Lambda(1405)$ [5](briefly explaining in the next paragraph). Unfortunately, statistics in experimental data seems poor and 2 π^0 in the final state cannot be distinguished kinematically each other. Recently, the $\gamma p \rightarrow K^+\pi^+\Sigma^-$ and $K^+\pi^-\Sigma^+$ reactions were measured at LEPS/SPring-8 [6]. Although the statistics is limited, they claimed the interference between the I=1 and I=0 amplitudes. The $K^-d \rightarrow \pi^+\Sigma^-n$ reaction was reported [7], which shows a clear peak at the $\Lambda(1405)$ mass region. This reaction seems promising to study $\Lambda(1405)$. The other decay mode, particularly $Y^* \rightarrow \pi^0\Sigma^0$, must be measured. In short, experimental study on $\Lambda(1405)$ is not yet satisfactory.

A repulsive shift of K^-p atomic state at 1s energy region [8] arises an interesting discussion of deeply bound kaonic nuclear states, where Λ (1405) is interpreted as a bound state of $\bar{K}N$ system with the binding energy of as deep as 27 MeV [9]. On the other hand, a chiral unitary model calculation claims that Λ (1405) may consist of two components in the coupled-channel $\bar{K}N$-$\pi\Sigma$ system [10]. Namely, poles coupled to the $\pi\Sigma$ state and $\bar{K}N$ state are suggested at different positions, (1390 – 132i) MeV and (1426 – 32i) MeV, respectively [11]. As a consequence, the resonance position of the $\bar{K}N \rightarrow \pi\Sigma$ channel sits at about 1420 MeV and the binding energy is as shallow as 15 MeV. This situation obviously affects the property of the deeply bound kaonic nuclear states. In order to clarify which picture is valid, decomposition of Λ (1405) states coupled to $\bar{K}N$ is of essentially importance. Since Λ (1405) lies below the $\bar{K}N$ threshold and has no decaying channel coupled to $\bar{K}N$, it is vital to investigate a $\bar{K}N$ collision process in a virtual state.

We therefore intend to employ a (K^-,n) reaction on the deuterium target to produce Λ (1405). These reactions are expected to enhance a virtual $\bar{K}N$ scattering process [12], where a K^- beam kicks a neutron out of the deuteron target in a forward angle and is slowing down to form a Λ (1405) with a residual nucleon, as shown in Fig. 1. It is important to measure all the $\Sigma^+\pi^-$, $\Sigma^-\pi^+$, and $\Sigma^0\pi^0$ final states so that the isospin structure of the produced hyperon resonance state can be decomposed. The primary goal of the present study is exclusively to show the position and the width (for the line shape information) of the Λ(1405) resonance produced in the $\bar{K}N \to \pi\Sigma$ channel.

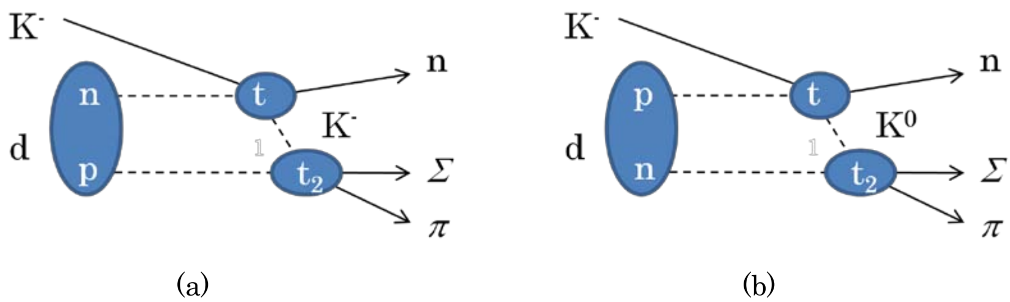

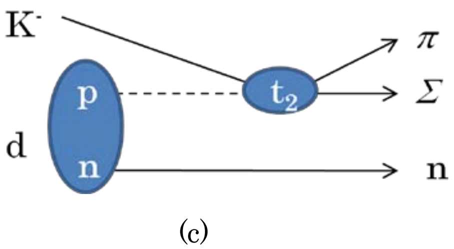

Fig. 1: (K^-,n) Reaction Diagram. The amplitude (a) is expected to be dominant at a neutron forward direction.

2. Experiment

We measure missing mass spectra in the inclusive (K^-,n) reaction on the deuteron target. In coincidence with each reaction, decay charged particles in the decay process will be measured, identifying as follows:

$\Lambda(1405) \to \pi^+\Sigma^- \to \pi^+\pi^- n$ (33%)

$\to \pi^-\Sigma^+ \to \pi^-\pi^+ n$ (16%), $\pi^-\pi^0 p$ (17%)

$\to \pi^0\Sigma^0 \to \pi^0\pi^- p$ (21%), $\pi^0\pi^0 n$.

Possible background processes are as follows:

$\Sigma(1385)^* \to \pi^+\Sigma^- \to \pi^+\pi^- n$ (6%),

$\to \pi^-\Sigma^+ \to \pi^-\pi^+ n$ (3%), $\pi^-\pi^0 p$ (3%),

$\rightarrow \pi^0\Lambda \rightarrow \pi^0\pi^-p$ (56%), $\pi^0\pi^0n$,

and incoherent processes. Number in parenthesis shows a branching ratio in each hyperon resonance.

Experimental setup is to comprise as follows:

1) incident kaon beam counters and momentum analyzing spectrometer,
2) liquid deuterium and ^{3}He targets,
3) scattered neutron and deuteron counters and their momentum analyzer at a forward angle, and
4) decay particle counters and momentum analyzer.

The E15 setup satisfies above components. Therefore, we assume to use the setup in the present study. Some additional detectors necessary for the present purpose will be described below.

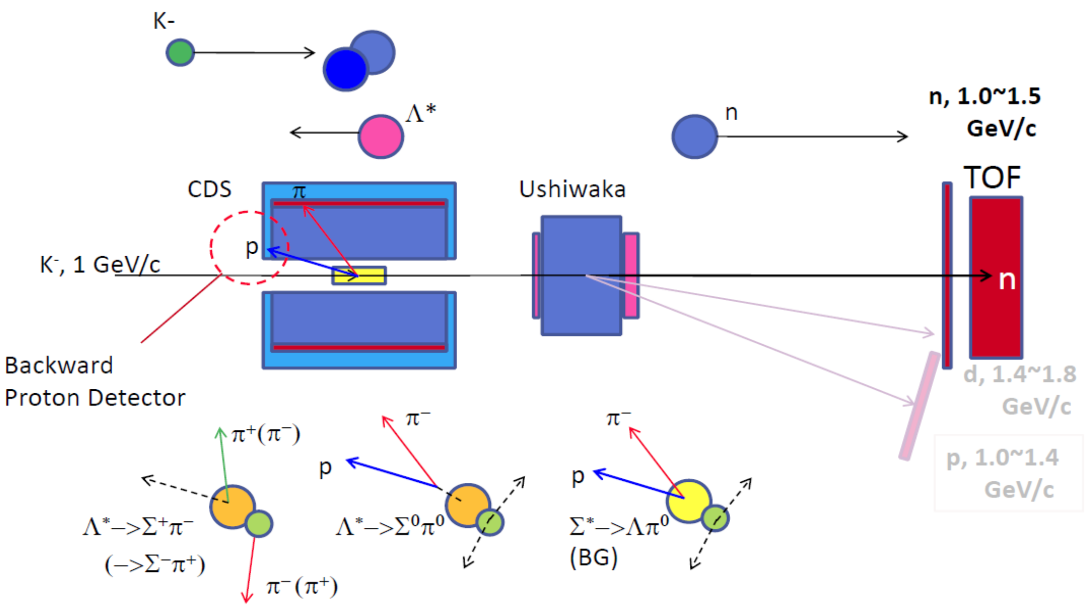

Fig. 2: Conceptual layout of the present experimental setup. It is almost same as the E15 setup. Backward proton detectors will be added for the present experiment. See also Fig. 5.

2.1 Summary of E15 setup

Schematic drawing of the E15 setup [13] is illustrated in Fig. 2. Since the reaction scheme is same as that of E15, the detector system and trigger condition is almost the same as that of E15. Because the requested beam rate is one order of magnitude less than that of E15, requirement for the trigger condition would not be very tight.

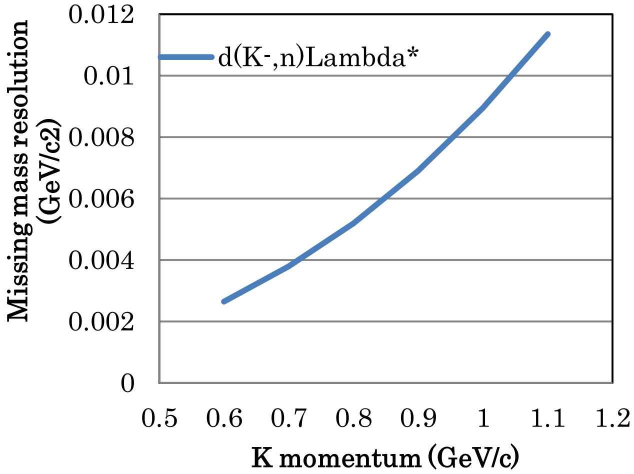

Fig. 3: Missing mass resolution as a function of the kaon momentum in σ.

2.2 Time of Flight detectors for scattered neutron

Neutron counters of the E15 setup will be used to measure scattered neutron momentum. The flight length is typically 15 m. Time resolution of 120 ps is expected for the TOF counters. The thickness (5cm) of the neutron counters and the vertex resolution (3 mm for $\pi^{\pm}\Sigma^{\mp}$ mode, 2cm for $\pi^0\Sigma^0$ mode) at the target affect measurement of neutron velocity because they cause ambiguity of the flight length. In total, the missing mass resolution is estimated to be 9 MeV/c^2 in the case of d(K^-,n)Λ(1405) at incident K^- momentum of 1 GeV/c. The missing mass resolution is plotted as a function of the incident K^- momentum in Fig. 3.

2.3 Backward decay particle counters

In the present reactions, Λ(1405) is recoiled at a backward angle. Among the decay particles, the angular distribution of pions is kept isotropic but that of protons is relatively boosted backward. Typical angular distributions of pions and protons are shown in Fig. 4. It is shown that detection of backward proton is necessary to measure Λ(1405) → $\pi^0\Sigma^0$ mode efficiently. Since the backward proton has a small transverse momentum, the solenoid magnetic field little affects the proton trajectory. A momentum of the proton will be measured by the time of flight.

A backward decay particle counter, BPD2, will be placed 45 cm upstream from the target center, which covers from 160 to 180 degrees, as illustrated in Fig. 5. Technical issue of the counter development is to realize a fast timing measurement in the strong

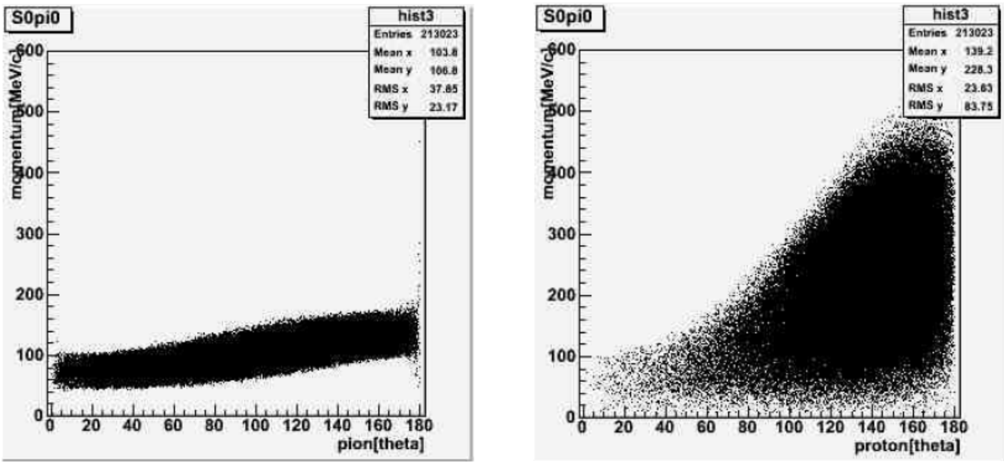

Fig. 4: Angular and momentum distribution of pions (left) and protons (right) in the $\pi^0\Sigma^0$ decay mode from produced hyperon resonance at 1400 MeV/c^2.

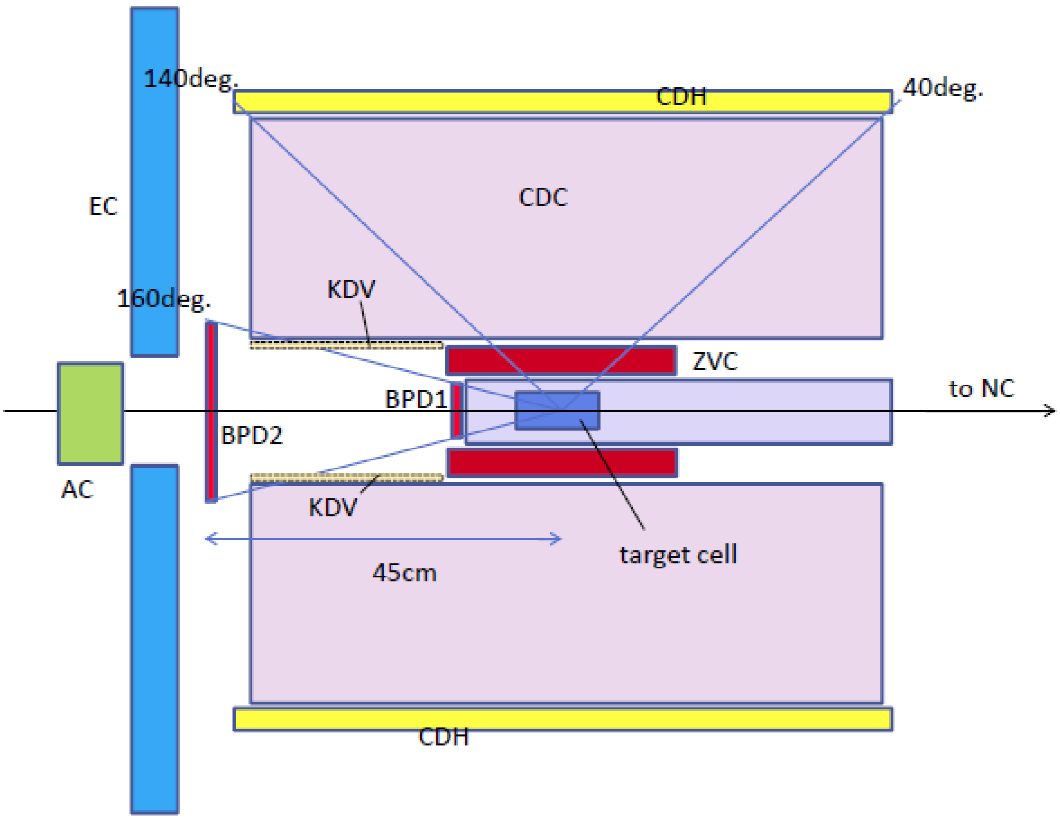

Fig. 5: A layout plan of the backward proton detectors (BPDs) in the CDS. AC: Aerogel counter for beam K^-, CDH: Hodoscope for charged decay particle, CDC: Cylinderical drift chamber, and ZVC: Z vertex chamber. KDV: Kaon decay veto counters (will not be used in the present experiment).

magnetic field of 5 kGauss. At this moment, we consider a use of MPPC. Recent year, an MPPC with a large sensitive area of 3 mm by 3 mm becomes available, which opens a possible use for photon sensors of plastic scintillator hodoscopes. A time resolution as good as 200 ps or better can be expected.

Another counter, BPD1, will be placed just in front of the target vessel. This counter will play two major roles. One is to recognize a charged beam at the closest distance from the target. In E15, there is no beam defining counter near the target. There is a distance of more than 60 cm from the last beam defining counter T0 to the target. As a result, number of kaons decay before the target, which may arise fake trigger condition similar to the (K^-, n) reaction. Therefore, annular shape of a kaon decay veto counter (KDV) is proposed to place along inner surface of CDC. KDV vetoes a charged particle emitted at the large angle from the beam direction from a kaon decay, while the other neutral particle is emitted at the forward angle, to reduce fake triggers from kaon decays. However, KDV will veto a certain amount of backward protons. Therefore, we propose to place a charged particle counter, BPD1, as close as the target, instead. BPD1 requires a charged particle at the forward angle. As far as the fake trigger arising from dominant two body kaon decays, BPD1 will play almost same function as of KDV.

The other role of BPD1 is to help to determine the vertex point. As is already mentioned, the vertex point cannot be determined very well in the case of $Y^* \rightarrow \pi^0\Sigma^0$ mode. Only a decay vertex of Λ suggests the Y^* produced point. However, the finite decay length causes ambiguity of the reaction vertex. This is estimated to be about 2 cm from the measured Λ decay vertex, which affects the TOF measurement of a neutron. A fine grain detector with a thin material is required for design of BPD1. A thin segmented scintillator hodoscopes with MPPC is a possible candidate at present.

2.4 Identification of the decay modes: $\Lambda(1405) \rightarrow \pi^+\Sigma^-$ or $\pi^-\Sigma^+$

Final $\pi^+\Sigma^-$ or $\pi^-\Sigma^+$ state would be identified by detecting 2 charged pion tracks with different charges. Both pions can be detected by CDS. Because we measure a 4 momentum of the recoiling hyperon resonance (Y^*) in the inclusive d(K^-,n) reaction, we obtain two missing masses with combining decaying Y^* and two pions, which corresponds to the invariant mass of π^-n or π^+n. As one of the combinations show a peak at the Sigma hyperon mass, we can identify which mode $Y^*\rightarrow\pi^+\Sigma^-$ or $\pi^-\Sigma^+$ takes place. Fig. 6 shows expected missing mass square spectra obtained from Y^* and one of detected charged pions. Missing mass square distributions in the case of choosing the other $Y^*\pi$ combination of a wrong decay mode are overlaid in the figures. As is indicated with vertical lines and arrows in Fig. 6, one can set a window to identify the correct decay

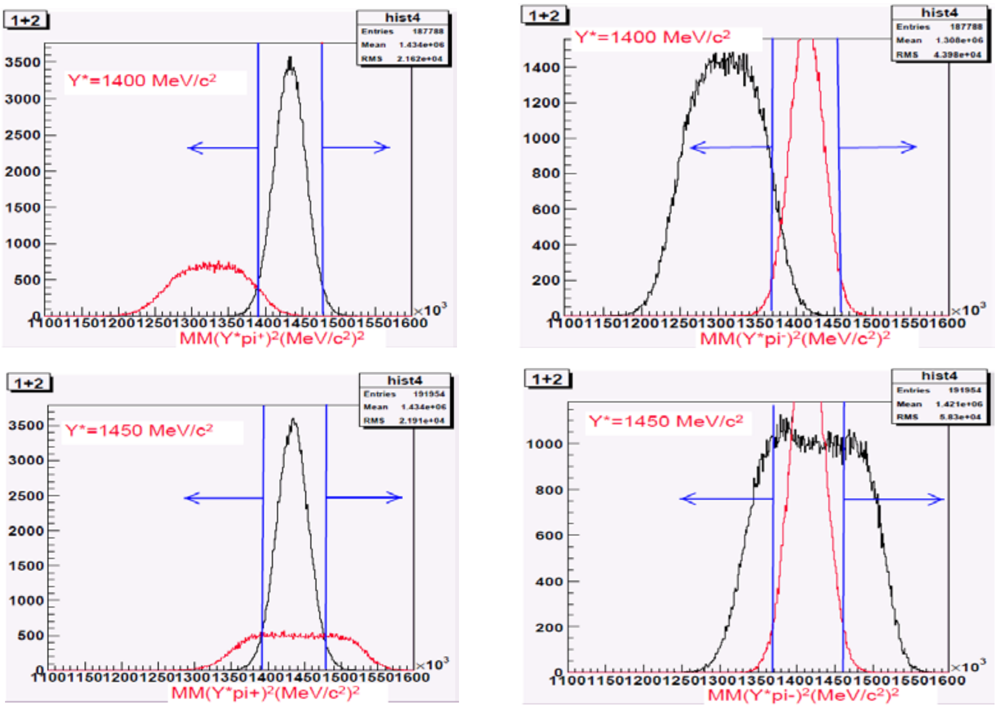

Fig. 6: Missing mass square spectra of $Y^*\pi^+$ and $Y^*\pi^-$, which corresponding to the invariant masses of π^-n and π^+n in the $\pi^+\Sigma^-$ (left) and $\pi^-\Sigma^+$ (right) decay modes, where Y^* represents a produced hyperon resonance. A correct pair of pion and neutron shows a clear peak at the corresponding Sigma hyperon mass square. Missing mass square distributions in the case of choosing the other combination of a wrong decay mode are overlaid in the figures. Here, the ratio of $\bar{K}N \rightarrow \pi^+\Sigma^-$ to $\bar{K}N \rightarrow \pi^-\Sigma^+$ is assumed to be 1. The windows indicated by arrows identify the decay mode.

mode. As is shown in Fig. 6, the missing mass spectra for the correct combination and the wrong one become close each other as the mass of Y* is greater than 1400 MeV/c². Therefore, a window to exclude around a sharp peak at the Sigma hyperon mass can reduce contamination (or misidentification) instead of gating the peak.

In this manner, the detection efficiency for each decay mode is plotted as a function of produced Y^* mass in Fig. 7. The event ratios to misidentify the decay mode are also plotted in the figure. Here, the ratio of $\bar{K}N \rightarrow \pi^+\Sigma^-$ to $\bar{K}N \rightarrow \pi^-\Sigma^+$ is assumed to be 1. We found the efficiency for the charged decay mode is sufficiently large at the interesting mass region of around 1400 ~1440 MeV/c.

2.5 Identification of the decay modes: $\Lambda(1405) \rightarrow \pi^0\Sigma^0$

$\Lambda(1405) \rightarrow \pi^0\Sigma^0 \rightarrow \pi^0\gamma\Lambda \rightarrow \pi^0\gamma\pi^-p$, Competing processes are $\Lambda(1405) \rightarrow \pi^-\Sigma^+ \rightarrow \pi^-\pi^0p$,

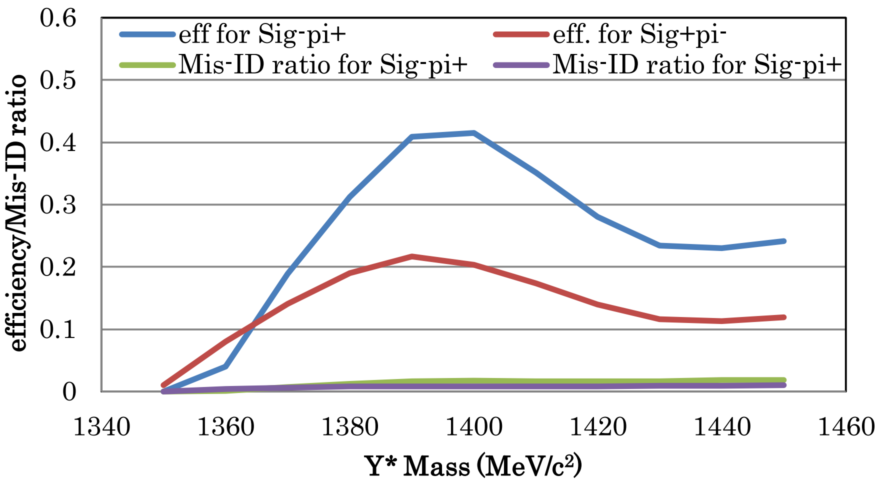

Fig. 7: Estimated detection efficiencies for $\pi^+\Sigma^-$ and $\pi^-\Sigma^+$ decay modes identified by π^+ and π^- as a function of hyperon resonance (Y*) mass produced by the d(K-,n) reaction. The event ratios to misidentify the decay mode are also plotted

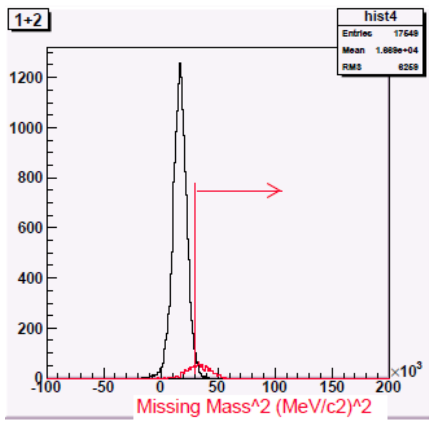

Fig. 8: Missing mass square spectrum of produced hyperon resonance and detected π^-p in the $\pi^0\Sigma^0$ decay mode at the produced Y* mass of 1400 MeV/c². Missing mass square in the $\pi^0\Lambda^0$ decay mode is also overlaid in the same plot.

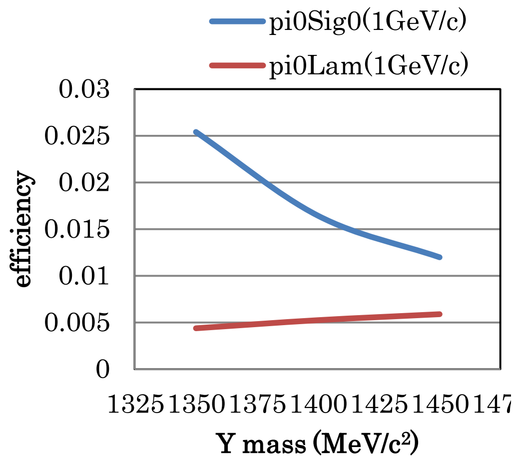

Fig. 9: Estimated detection efficiency for $\pi^0\Sigma^0$ decay mode identified by π^- and p as a function of hyperon resonance (Y*) mass produced by the d(K-,n) reaction.

$\Sigma(1385) \rightarrow \pi^-\Sigma^+ \rightarrow \pi^-\pi^0 p$, and $\Sigma(1385) \rightarrow \pi^0\Lambda \rightarrow \pi^0\pi^- p$. First two modes can be identified if the invariant mass of detected π^-p reproduces lambda. In order to separate the 3rd mode, we take missing mass for undetected neutral particles by employing detected π^-p and measured four momentum of produced Y*. Fig. 8 shows a typical missing mass

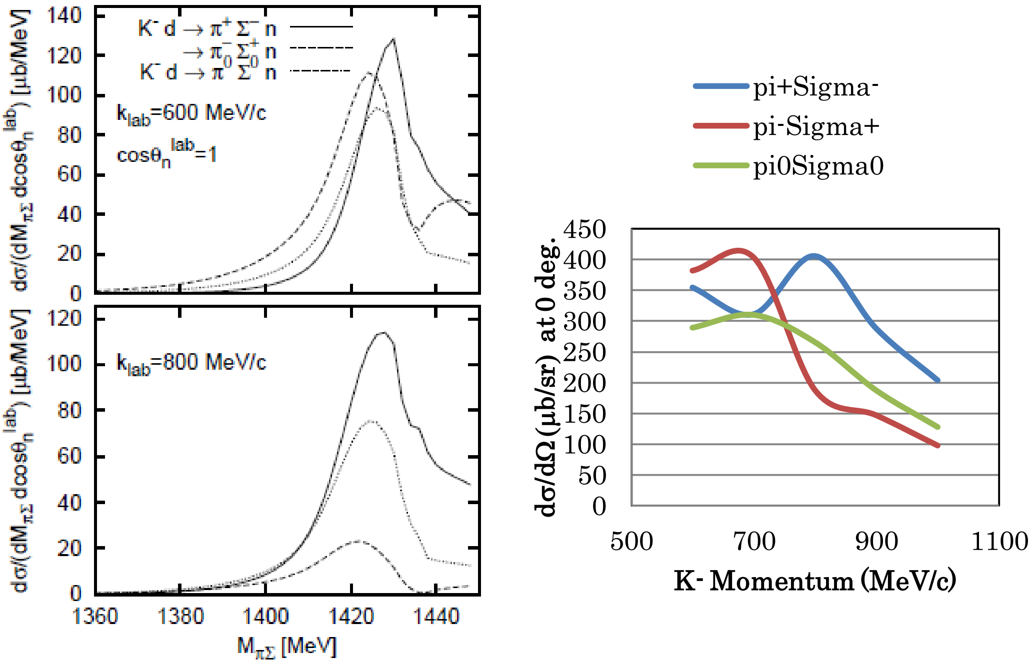

Fig. 10: Calculated reation cross sections by Chiral Unitary Model [12].

spectrum for the $\Lambda(1405) \rightarrow \pi^0\Sigma^0$ mode. The $\Sigma(1385) \rightarrow \pi^0\Lambda$ mode is overlaid in Fig.8. Here, the production ratio of $\Lambda(1405)$ to $\Sigma(1385)$ is assumed to be 1. The missing mass square of greater than 30000 (MeV/c^2)^2 may be selected as the $\pi^0\Sigma^0$ decay mode, as indicated by an arrow. The detection efficiency and contamination from the $\pi^0\Lambda$ mode for each decay mode is plotted as a function of produced Y^* mass in Fig. 9.

3. Yield Estimation

Fig. 10 shows calculated differential cross section based on chiral unitary model [12]. We estimate expected yield of each mode as follows.

$$Y = \mathrm{I_b} \times n_t \times \frac{d\sigma}{d\Omega} \times \Delta\Omega \times \varepsilon_\mathrm{R} \times \varepsilon_\mathrm{M} \times \varepsilon_\mathrm{A}$$

Here, I_b and n_t are a K- beam intensity and the number of target nuclei. The reaction cross section is denoted by $d\sigma/d\Omega$. $\Delta\Omega$ is a solid angle for scattered n in the (K-,n) reaction. The efficiencies to reconstruct the hyperon resonance production reaction and to identify hyperon resonance decay mode are represented by ε_R and ε_M. The efficiencies for DAQ and neutron detection are taken into account in ε_R. Analysis efficiency of $\varepsilon_\mathrm{A} = 0.8$ is assumed in the present estimation.

The beam intensity is expected to be 2x10^5 K^- per spill (6 second repetition) at 1 GeV/c. This is based on estimation by using Sanford-Wang formula at 30 GeV. Primary beam power of 27 kW is assumed to be irradiated on a nickel 54 mm thick target. A thickness of the deuteron target is assumed to be 8 cm for the yield estimation, since it is close to the range for the backward proton ~300 MeV/c in the deuteron. Use of the 12 cm long target cell, which will be used in E15, may be no problem, but contribution from downstream 4 cm may not be expected very much. Above mentioned parameters are listed in Table 1. The estimated yields for the modes to $\pi^{\pm}\Sigma^{\mp}$ and $\pi^0\Sigma^0$ are found to be respectively ~19200, ~4800, and ~350 events in 120 shifts.

Table 1: Yield estimation and used parameters.

	mnemonic		
Intensity	I_b	2.E+5 ppp	30GeV-27kW (6 s)
# of target nuclei	n_t	4.1E+23	D:8cm, 0.169g/cc
Reaction X section at p_K = 1 GeV/c (from Ref. [12])	$d\sigma/d\Omega$	220 μb/sr 97 128	$\Lambda\to\pi^+\Sigma^-$ $\Lambda\to\pi^-\Sigma^+$ $\Lambda\to\pi^0\Sigma^0$
Solid angle	$\Delta\Omega$	0.020 sr	
Reconstruction eff. DAQ Beam tracking Neutron detection	ε_R	0.24	 0.9 0.9 0.3
Decay mode eff. (including. B.R.)	ε_M	0.32 0.16 0.015	$\Lambda\to\pi^+\Sigma^-\to\pi^+\pi^-n$ $\Lambda\to\pi^-\Sigma^+\to\pi^-\pi^+n$ $\Lambda\to\pi^0\Sigma^0\to\pi^0\pi^-p$
Analysis eff.	ε_A	0.8	
Yield	Y	~19200 ~4800 ~350	120 shifts 120 shifts 120 shifts

4. Budget Request

Most of setup will be prepared by E15. New items for the present experiment are limited, as follows.

1) BPD1, 2: ~5000k¥.

2) Deuterium: expected to be prepared by RIKEN for another experiment (stopped K^-,n).

3) Running Cost for the experiment.

Chamber Gases, Standard Electronics modules, etc.

5. Schedule

The R&D work for BPDs will be completed this year. The present experiment can be done after the E15 experiment gets ready. It is natural that the present experiment will be successively scheduled after the E15 experiment. Currently, we understand that E17 will be done first at K1.8BR. Engineering run will start from coming fall beam time. E17 will be ready to start experiment in the next fiscal year, JFY2010. E15 as well as the present experiment is expected to be ready by the end of E17.

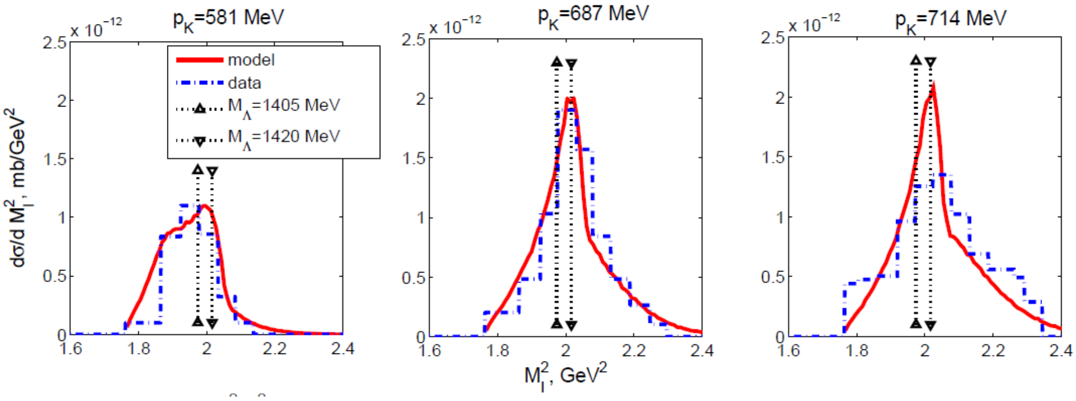

Fig. A1: Reconstructed missing mass square spectra from observed $\pi^0\Sigma^0$ are shown, which correspond to the Λ(1405) state. Lines are calculations based on the chiral unitary model [5] and histograms are experimental data [4].

Appendix

A. Breif description of experimental situations on Lambda(1405)

The existence of Lambda(1405) is established as a 4-star hyperon resonance in the Review of Particle Physics by the Particle Data Group [1]. According to the review, its mass and width are obtained as 1406.4±4 MeV/c² and 50 ±2 MeV. The review adopted the values obtained using M-matrix analysis by R. H. Dalitz *et al.* [2] based on the K^-p → ($\pi^-\Sigma(1670)^+$ → $\pi^-\pi^+\Lambda(1405)$) → $\pi^-\pi^+\pi^-\Sigma^+$ → $\pi^-\pi^+\pi^-\pi^+n$ reaction data samples in the hydrogen bubble chamber at the kaon momentum of 4.2 GeV/c [3]. Processes of $\Sigma(1670)^+$ production and its decay into $\pi^+\Lambda(1405)$ are however unclear. It seems difficult to discuss the $\bar{K}N$ coupling to Λ(1405) by this process.

On the other hand, recent analysis based on the chiral unitary model claims that Λ(1405) may has two pole structure; one is the πΣ state and the other the $\bar{K}N$ state. Magas et al. compared their calculation [5] with the Λ(1405) spectra reconstructed from observed $\pi^0\Sigma^0$ in the K^-p → $\pi^0\pi^0\Sigma^0$ reactions at the K^- momenta of 581, 687, and 714 MeV/c [4]. (The experiment in Ref. [4] reported another data set at the K^- momentum of 750 MeV/c.) Fig. A1 shows the calculated line shapes of Λ(1405), suggesting a peak at around 1420 MeV/c. The theory seems to fit the above-mentioned experimental data. Final state of $\pi^0\Sigma^0$ guarantees production of the Λ(1405) state of the isospin I=0. However, unfortunately, the experiment cannot distinguish two π^0 because they are kinematically very similar. The spectra suffer from unavoidable contamination from wrong combinations of $\pi^0\Sigma^0$, although the theory took this situation into consideration.

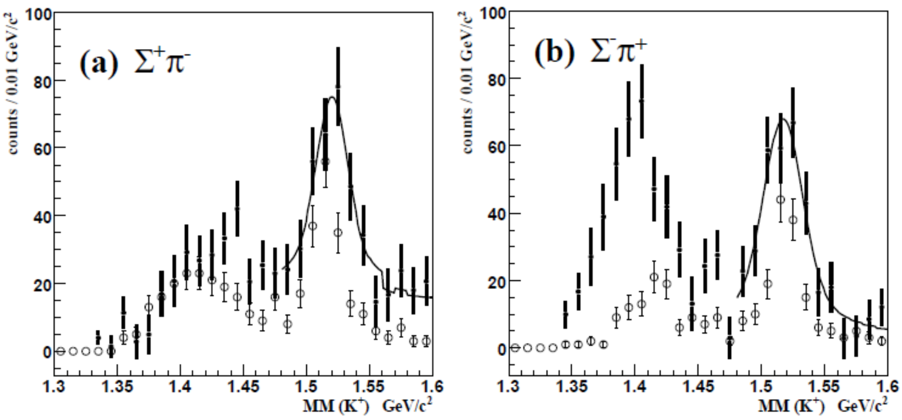

Fig. A2: Missing mass spectra in coincidence with final $\pi^+\Sigma^-$ (a) and $\pi^-\Sigma^+$ (b) states were measured [6]. The figures show different shapes and yields, which are considered due to the interference term.

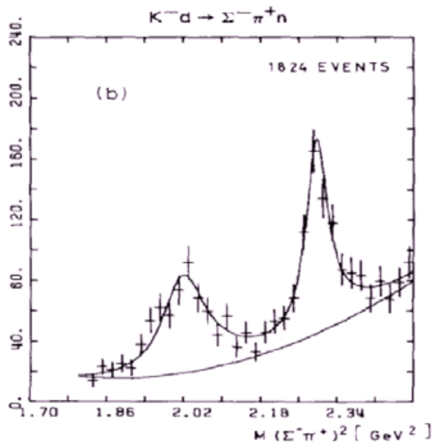

Fig. A3: Invariant mass square spectrum reconstructed from observed $\pi^+\Sigma^-$ was measured in the (K$^-$,n) reaction on the deuteron target [7].

Magas et al. also claimed that the produce Y* spectrum in a different experiment by the $\pi^- p \rightarrow K^0\pi\Sigma$ reaction [14] is fit with their calculation, where a peak position seems to be consistent with a pole position corresponding to the $\pi\Sigma$ state.

Recently, $\Lambda(1405)$ formation via the (γ, K$^+$) reaction on hydrogen was reported by the LEPS collaboration at Spring-8 [6]. Missing mass spectra in coincidence with final $\pi^+\Sigma^-$ and $\pi^-\Sigma^+$ states were measured separately, as shown in Fig. A2. The spectra show different shapes and number of counts. This is considered due to the interference term of the I=0 amplitude with the I=1 one, as indicated in chiral unitary model theory [15]. It seems that the observed spectra are consistent with those observed in Ref. [3]. They

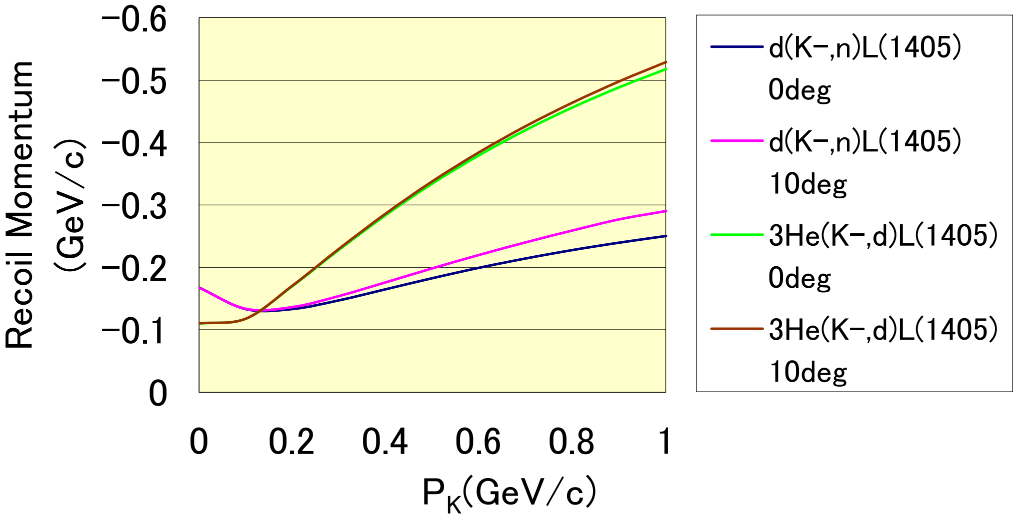

Fig. B1: Recoil momentum of Λ(1405) produced by the d(K^-,n) and ^{3}He(K^-,d) reactions as a function of incident K^- momentum.

also reported strong energy dependence on the production rate of Λ(1405), shown in the decomposed inclusive spectra at different gamma energy regions. On the other hand, the inclusive spectra suggest that a large fraction of the Σ^*(1385) productions. More experimental studies using the (γ, K^+) reaction are necessary, particularly in statistics.

The d(K^-,n) reaction at the K^- momentum region of 673~834 MeV/c was measured in the deuteron bubble chamber [7]. This experiment did not measure the scattered neutron. However, it is interesting that invariant mass spectrum reconstructed from observed $\pi^+\Sigma^-$ shows a peak at around 1420 MeV/c, as shown in Fig. A3, which seems a consistent with a theoretical calculation based on the chiral unitary model [12]. Therefore, it is important to measure the other different charge mode decays, $Y^* \rightarrow \pi^-\Sigma^+$ and $\rightarrow \pi^0\Sigma^0$. The present experiment is expected to improve almost two order of magnitude in statistics of $Y^* \rightarrow \pi^+\Sigma^-$.

B. Comment on the measurement of the ^{3}He(K^-,d) reaction

We intended to measure the (K^-,d) reaction on the ^{3}He target, during the E15 experiment. This reaction can also produce the Lambda(1405) hyperon. The purpose of the measurement can be summarized as follows.

1) This measurement would be a pilot experiment of the present (K^-, n) reaction on the

deuteron target. The detection of the decay mode of Y^* to $\pi^{\pm}\Sigma^{\mp}$, $\pi^0\Lambda$ as well as $\pi^0\Sigma^0$ can be tested.

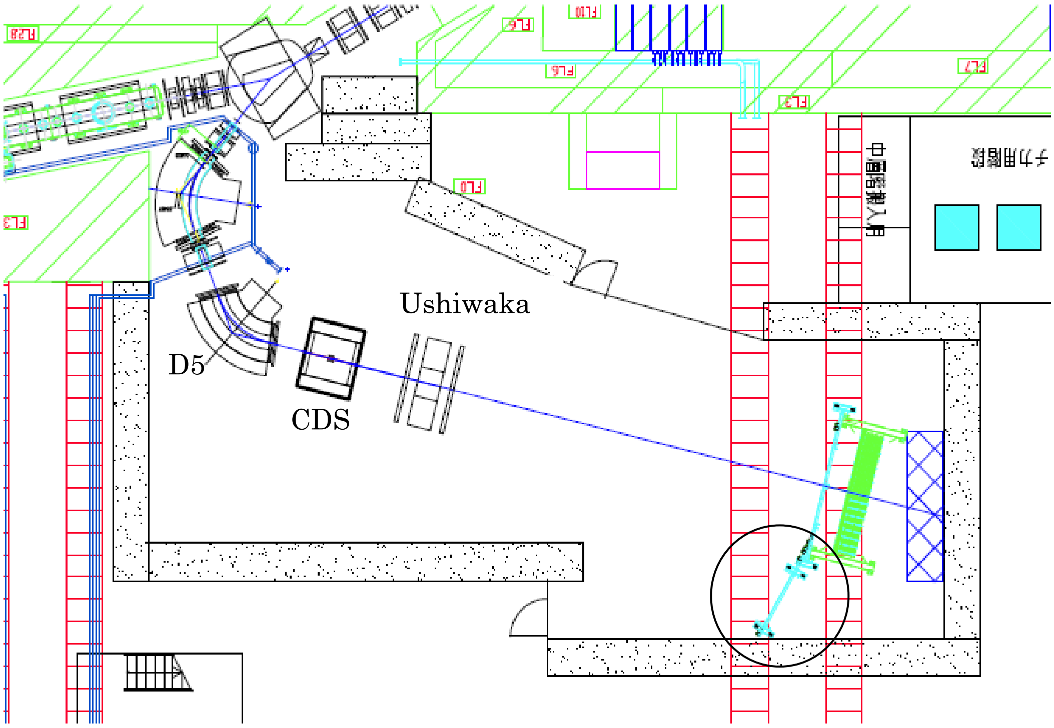

Fig. B2: K1.8BR layout. Location of scattered deuteron detector is indicated by a circle in the figure. A momentum of the scattered charged particle is obtained by measured time of flight. Tracking chambers, to be placed at the entrance and the exit of the Ushiwaka magnet, are being prepared to correct the deuteron flight path.

2) The reaction is interesting since the recoil momentum of the produced hyperon resonance, Y^*, is almost twice greater than that of the (K^-,n) reaction on D (Fig. B1). The spin, isospin states of produced Y^* may be different. For example, P-wave contribution to the $\bar{K}N$ scattering is expected to increase and the Σ^* production is increase. This information would be helpful to understand the reaction mechanism of $\bar{K}N \rightarrow \pi\Sigma$ below $\bar{K}N$ threshold.

The experimental requirement is to prepare the detector system for the scattered deuteron. Fortunately, another experimental proposal to measure $^3He(K^-,p)$ reaction is submitted [16], which is going to prepare the scattered proton detector, as shown in Fig. B2. This proton detector is compatible to the deuteron detector.

The (K^-, d) reaction is not well known. Theoretical prediction is difficult since two-nucleon correlation must be taken into account at least in the final state. Naïve estimation is two order of magnitude smaller than the (K^-, n) reaction. If incident kaon can directly look at a correlated two nucleon component like "quasi-deuteron" in a nucleus, the (K^-, d) reaction may be enhanced much. Experimental information is thus necessary.

References:

[1] C. Amsler *et al.*, "The Review of Particle Physics", Physics Letters **B667**, 1 (2008); Particle Data Group, http://ccwww.kek.jp/pdg/index.html.

[2] R. H. Dalitz and A. Deloff, J. Phys. G17, 289(1991).
Note on $\Sigma(1670)^+$: Σ hyperon resonance quoted here is appeared as $\Sigma(1660)+$ in this paper and Ref. [3]. However, it is quoted as an I=1, J=3/2$^-$ state, which is attributed to $\Sigma(1670)^+$ by recent PDG.

[3] R. J. Hemingway *et al.*, Nucl. Phys. B253, 742(1985).

[4] S. Prakhov et al., Phys. Rev., C70, 034605(2004).

[5] V.K. Magas, E. Oset, A. Ramos, Phys. Rev. Lett., 95, 052301(2005).

[6] M. Niiyama *et al.*, Phys. Review C78, 035202(2008).

[7] O. Braun *et al.*, Nucl. Phys. B129, 1(1977).

[8] M. Iwasaki *et al.*, PRL78 (1997) 3067.

[9] Y. Akaishi and T. Yamazaki, Phys. Rev. **C65**, 044005(2002);
Y. Akaishi and T. Yamazaki, Phys. Rev. **C76**, 044005(2002).

[10] T. Hyodo, D. Jido, and A. Hosaka, Phys. Rev. Lett. **97**, 192002(2006);
T. Hyodo, D. Jido and A. Hosaka, Phys. Rev. **D75**, 034002(2007).

[11] T. Hyodo and A. Weise, Phys. Rev. C**77**, 035204(2008);

[12] D. Jido, E. Oset, and T. Sekihara, "Kaonic production of $\Lambda(1405)$ off deuteron target in chiral dynamics", arXiv:0904.3410;
D. Jido, private communication, 2009.

[13] M. Iwasaki, T. Nagae *et al.*, J-PARC E15 proposal.
http://j-parc.jp/NuclPart/pac 0606/pdf/p15-Iwasaki.pdf

[14] D. W. Thomas et al., Nucl. Phys., B56, 15(1973).

[15] Nacher, E. Oset, H. Toki, and A. Ramos, Phys. Lett., B(455), 55(1999)

[16] H. Fujioka et al., J-PARC Proposal, July 2009.

Proposal for the J-PARC 50-GeV Proton Synchrotron
Revised in July, 2012

At the suggestion of PAC, the following addendum is attached to the P31 proposal. It is based on a reply for the 8th PAC recommendation for deferred P31 and the presentation at the 9th PAC.

Addendum

Below is the 8th PAC recommendation for deferred P31.

The PAC recognizes the importance of the physics of the proposed measurements. However, there are important questions which remain to be addressed by the proponent. The PAC recommends that this proposal be deferred and reconsidered after the following questions are answered:

1) How are the additional data going to accomplish the stated goals of the proposal? Can an I = 0 component of the spectra be extracted unambiguously?
2) Is the experimental setup suitable for the measurement of the Sigma0pi0 decay channel? Is it possible to discriminate the background of Sigma*(1385)–>Lambda pi0?

The proposed experiment is **aiming primarily to clarify whether $\Lambda(1405)$ is a $\bar{K}N$ resonant state** as predicted by the chiral unitary model or not. To accomplish this aim, we will measure the $\Lambda(1405)$ state via the (K^-,n) reaction to test whether the resonance appears at ~1420 MeV/c^2 as predicted by the chiral unitary model [1] or at ~1405 MeV/c^2 as deduced by Dalitz *et al.* [2]. This experiment will provide vital and most fundamental information on the longstanding argument of the deeply bound kaonic nuclear state. If the $\Lambda(1405)$ is interpreted as a $\bar{K}N$ resonant state, we may have to re-consider a quark configuration of the baryon resonances and the classification of their excitation spectra.

Because $\Lambda(1405)$ lies below the $\bar{K}N$ threshold, it is hard to realize direct coupling of $\bar{K}N$ to $\Lambda(1405)$ in the $\bar{K}N$ scattering in free space. The $\bar{K}N$ to $\Lambda(1405)$ coupling takes place only through a collision in a virtual state. The $d(K^-,n)$ reaction realizes $\bar{K}N$

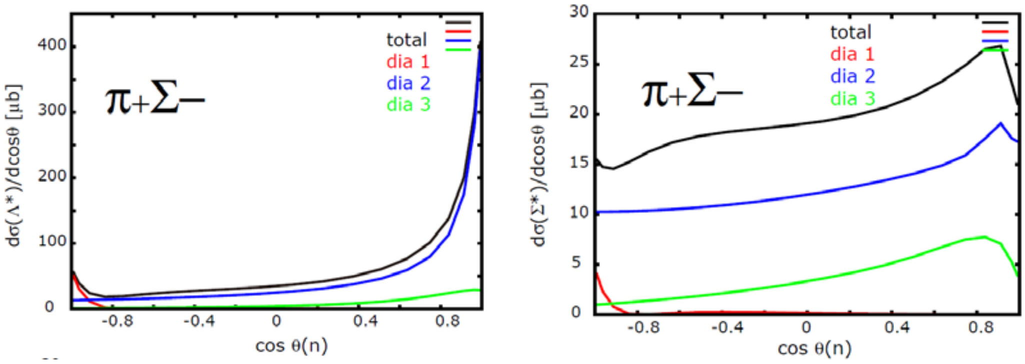

Fig. 1: Calculated angular distributions of the $\Lambda(1405)$ (left) and $\Sigma^*(1385)$ (right) cross sections as a function of the neutron scattering angle in the center of mass system in the $d(K^-,n)\Sigma^-\pi^+$ reactions at p_{K^-} = 800 MeV/c, where the P-wave component in $\bar{K}N$ scattering and explicit P-wave baryon components [3]. Diagrams 1, 2, and 3 correspond to those (c), (a), and (b) in Fig. 1 in the P31 proposal, respectively.

collision directly coupled to $\Lambda(1405)$ in an ideal way.

Recently, we re-confirmed that **the (K^-,n) reaction is an ideal reaction to form the $\Lambda(1405)$ state.** Fig. 1-left shows the differential cross section of the (K^-,n) reaction as a function of the neutron scattering angle, calculated by the chiral dynamics[3]. One can easily find that the cross section to produce **the $\Lambda(1405)$ state is strongly enhanced in the forward direction of the neutron scattering angle.** This can be simply understood as follows. In the d(K^-,n) reaction, the recoil momentum of the residual $\bar{K}N$ system is as low as 250 MeV/*c* at the incident kaon momentum of 1 GeV/*c*, which corresponds to only 160 MeV/*c* in the center of mass system. Because of the typical baryon size of 1 fm, the angular momentum introduced in the residual $\bar{K}N$ system is allowed to be less than $1 * 160/\hbar < 1$. Therefore, only the S-wave resonance, $\Lambda(1405)$, can be formed in the reaction. On the other hand, as shown in Fig. 1-right, no enhancement of the cross section at a neutron forward angle can be seen in the angular distribution of the P-wave $\Sigma^*(1385)$ resonance. In short, the d(K^-,n) reaction at a neutron forward angle produces $\Lambda(1405)$ dominantly.

The above-mentioned characteristic angular distributions of the hyperon resonances via the (K^-,N) reaction are worth of an additional comment. The d(K^-,p) reaction populates the $\Sigma^{*-}(1385)$ state. Comparison of the d(K^-,p) spectrum with the d(K^-,n) one, *i.e.* difference of the line shapes and the cross sections, at a nucleon forward angle would enhance a validity of the discussion. In the last PAC, Fujioka *et al.* proposed to place a proton TOF spectrometer system in the E15 setup in order to measure the ^{3}He(K^-,p)

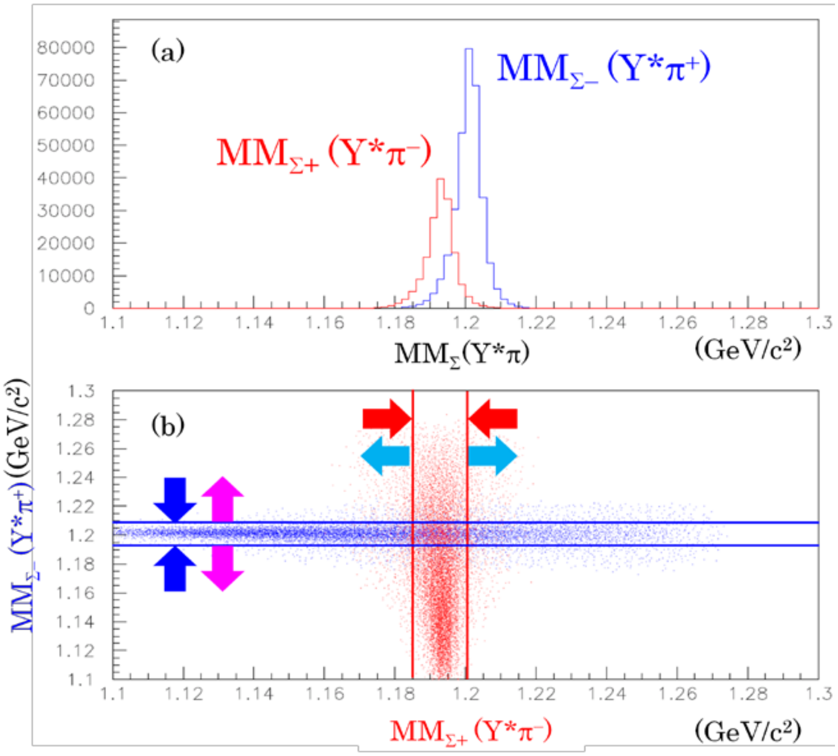

Fig. 2: Identification of the $\Sigma^+\pi^-$ and $\Sigma^-\pi^+$ decay modes from two different charged pion detections are shown in a Monte Carlo simulation. Missing mass distribution obtained from missing momentum measured in the d(K$^-$,n) reaction and that of one of detected pions are plotted in (b). Two loci corresponding to the two decay modes are clearly shown. (a) Missing mass distributions selected by the windows set in (b).

reaction [4]. The PAC considered that the proposed measurement is to be carried out as a part of E15. Therefore, we will take advantage of the existence of this detector and mix (K$^-$,p) triggered events in addition to (K$^-$,n) triggered ones.

Identification of each decay mode of the resonance produced is necessary. The identification of the final $\Sigma\pi$ states enriches the $\Lambda(1405)$ component in the d(K$^-$,n) spectrum because $\Lambda(1405)$ to $\Sigma\pi$ decay branching ratio is 100% while $\Sigma^*(1385)$ to $\Sigma\pi$ is only 12%.

Decomposition of the final $\Sigma^+\pi^-$ and $\Sigma^-\pi^+$ states is necessary to provide information on the difference of the line shapes and the magnitudes due to the interference term of the *I=0* amplitude to the *I=1* amplitude. The interference term is cancelled by adding the two spectra. The identification of the $\Sigma^+\pi^-$ and $\Sigma^-\pi^+$ states can be done by detecting two

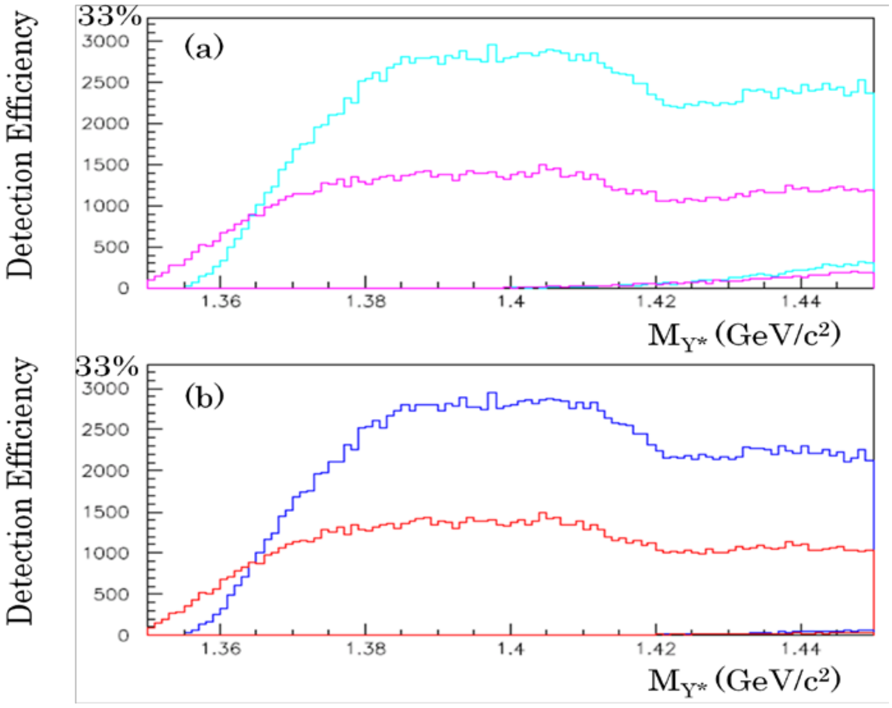

Fig. 3: Expected detection efficiencies and contaminations of the $\Sigma^-\pi^+$ (cyan/blue lines) and $\Sigma^+\pi^-$ (magenta/red lines) modes as a function of the produced hyperon mass (M_{Y^*}). Selected windows are defined in Fig. 2. (a) and (b) are for the events selected outside and inside of the windows, respectively.

different charged pions in the CDS system of the E15 experiment. Taking a missing mass of a Sigma hyperon with an associate pion from Λ(1405), we can identify which decay mode takes place, as shown in Fig. 2. Expected detection efficiencies and contaminations of the $\Sigma^-\pi^+$ and $\Sigma^+\pi^-$ modes are shown in Fig. 3. Therefore, we expect to **achieve the primary aim of measuring the position of the Λ(1405) state in the d(K^-,n) spectra in coincidences with $\Sigma^+\pi^-$ and $\Sigma^-\pi^+$ decay modes.**

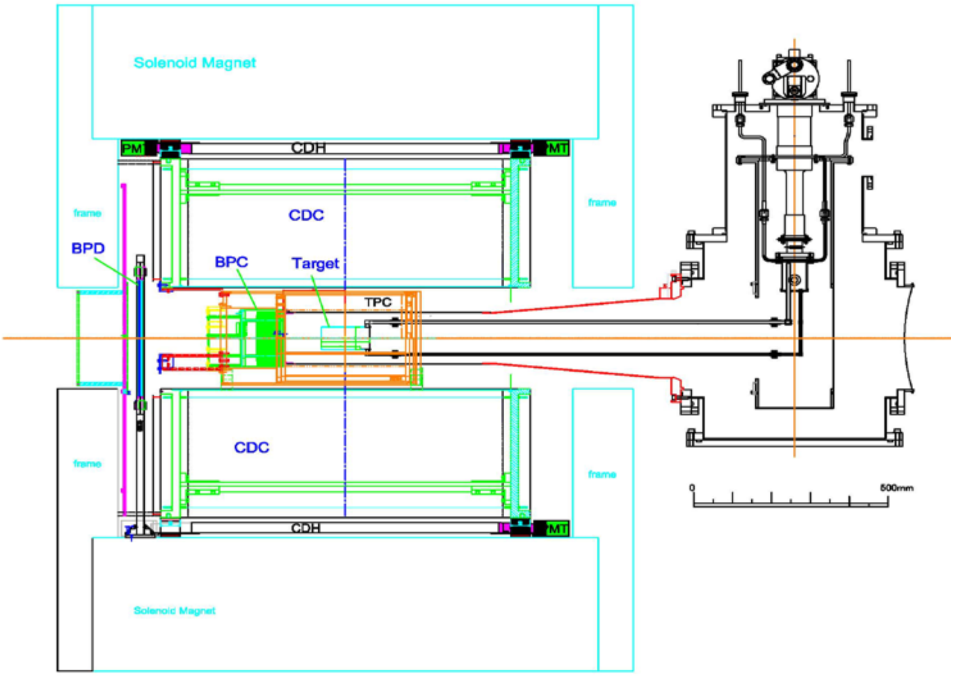

Fig. 4: Updated setup around the target for E31 is illustrated. Scintillator hodoscopes (BPD) and multi-wire drift chamber (BPC) are additionally placed in the CDS system in order to detect protons emitted from the Λ(1405) states.

Identification of the final $\Sigma^0\pi^0$ state is necessary to provide information on the *I=0* amplitude in the d(K-,n)Σπ reaction cross section. The identification of this decay mode will be done by detecting $p\pi^-$ in the decay chain of $\Sigma^0\pi^0 \to \Lambda\gamma\pi^0 \to p\pi^-\gamma\gamma\gamma$ in coincidence with the (K-,n) reaction. Σ*(1385) has a similar decay chain of $\Lambda\pi^0 \to p\pi^-\gamma\gamma$ and is a possible source of contamination to the $\Lambda(1405) \to \Sigma^0\pi^0$ mode. One needs to identify the two decay modes in the difference of the missing mass spectrum of $\gamma\pi^0$ from that of π^0. Due to the limited energy resolution, the Σ^* decay mode is contaminating to the Λ(1405) one at the level of 1/3 at around 1400~1420 MeV/c² in the missing mass spectrum if the production ratio of Λ(1405) to Σ^* is comparable as is assumed in the proposal (Fig. 9 in the proposal). However, **once it is shown that the production ratio is very much enhanced in the d(K-,n) reaction as is described above, the contamination of the Σ^* to $\Lambda\pi^0$ mode to the Λ(1405) to $\Sigma^0\pi^0$ mode would be very much reduced.**

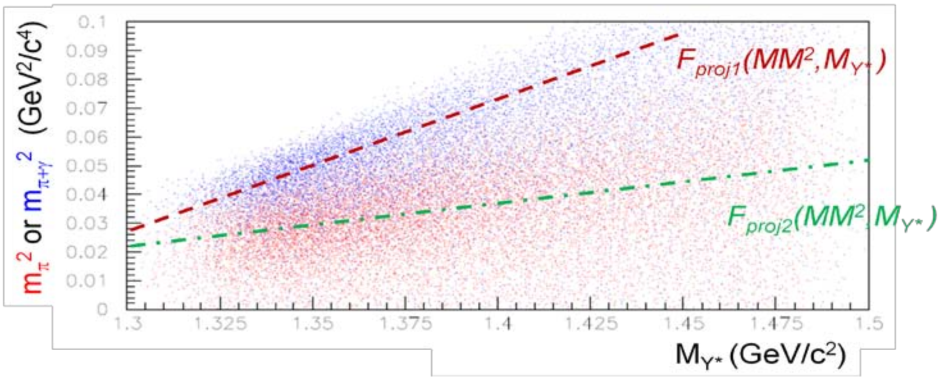

Fig. 5: Missing mass distribution obtained from proton and pion in the decay of the hyperon state produce by the d(K-,n) reaction, as a function of the produced hyperon mass (M_{Y*}) is shown. Proton and pion are detected by BPC/BPD and CDC/CDH, respectively. Two decay modes of $\Sigma^0\pi^0$ (blue) and $\Lambda\pi^0$ (red) assuming in an equal rate are plotted. We define projection functions along dashed and dash-dot lines.

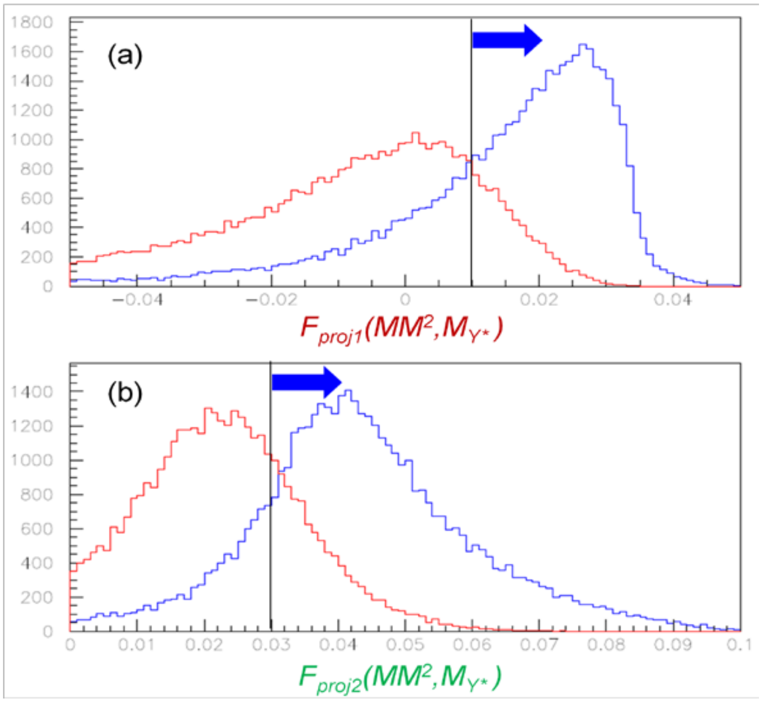

Fig. 6: Distributions of the projection functions, F_{proj1} and F_{proj2}, defined in Fig. 4 are shown in (a) and (b), respectively. Two decay modes of $\Sigma^0\pi^0$ (blue) and $\Lambda\pi^0$ (red) are partly overlapped each other. We select the regions of F_{proj1} >0.01 and F_{proj2}>0.03 to estimate the detection efficiency of the $\Sigma^0\pi^0$ mode and the contamination of the $\Lambda\pi^0$ mode.

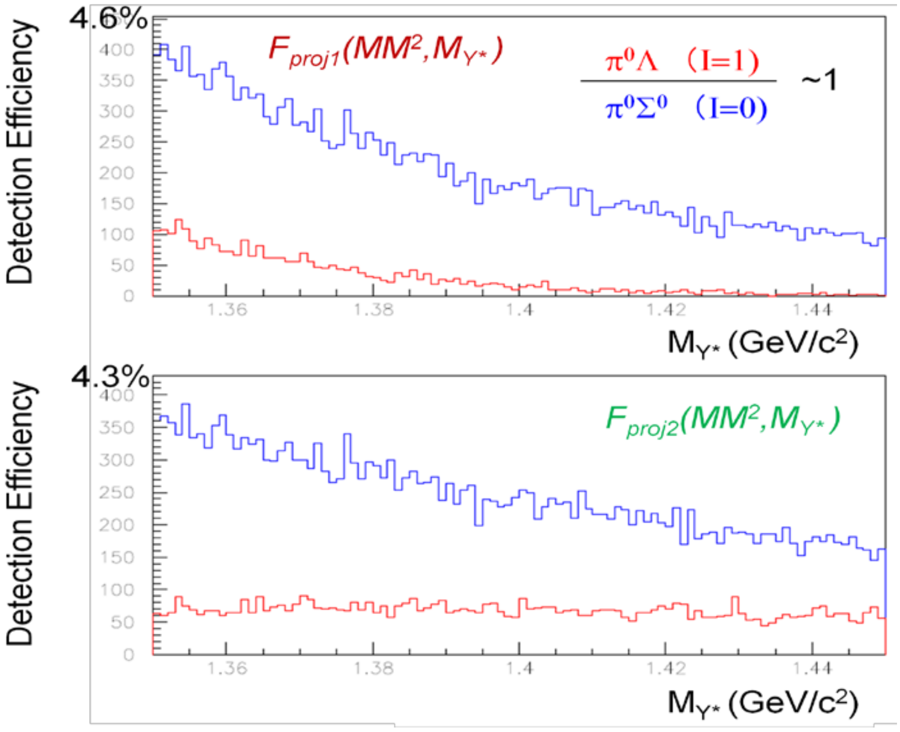

Fig. 7: Expected efficiencies (blue lines) of the $\Sigma^0\pi^0$ mode and contaminations (red lines) of the $\Lambda\pi^0$ mode as a function of the produced hyperon mass (M_{Y^*}). Selected regions of the projection functions are defined in Fig. 5.

As for the primary aim to fix the location of the Λ(1405) resonance produced via a $\bar{K}N$ collision, it will be accomplished by measuring the d(K^-,n) spectra through the final $\Sigma^+\pi^-$ and $\Sigma^-\pi^+$ states. The result of the measurement would shed light on the structure of Λ(1405), and give a big impact to the arguments on the deeply bound kaonic nuclear states.

We discussed about identification of the Λ(1405) to $\Sigma^0\pi^0$ mode by measuring negative pion and proton through the d(K^-,n) reaction. Particularly, **contamination of the Σ*(1385) to $\Lambda\pi^0$ mode may be much reduced due to possible enhancement of Λ(1405) production by the d(K^-,n) reaction at a neutron forward angle.** We will prepare to measure the Λ(1405) to $\Sigma^0\pi^0$ mode in order to obtain decomposed information on the magnitude of the *I=0* amplitude in the d(K^-,n) reaction.

In the d(K^-,n) reaction, produced Y* is emitted backward with a recoil momentum of ~250 MeV/*c*. The decay proton is rather emitted to the backward direction. We propose to place scintillator hodoscopes (BPD) to measure the velocity of the backward proton.

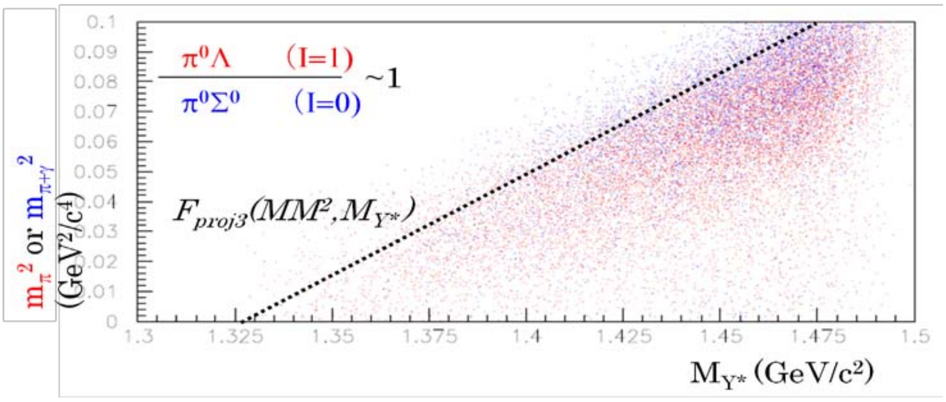

Fig. 8: Same as Fig. 4 but for the proton and pion detected only by CDC/CDH. We define a projection function along dotted line.

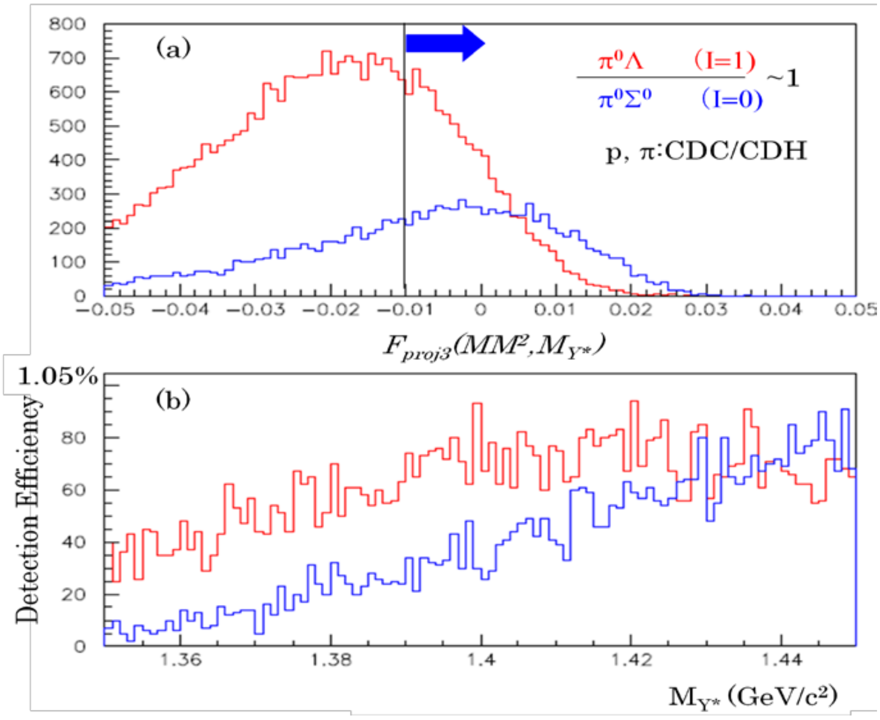

Fig. 9: (a) Distributions of the projection functions of the $\Sigma^0\pi^0$ (blue) and $\Lambda\pi^0$ (red) modes. (b) Expected efficiency and contamination of the $\Sigma^0\pi^0$ (blue) and $\Lambda\pi^0$ (red) modes detected only by CDC/CDH.

In addition, a multi-wire drift chamber (BPC) will be placed just before the target, in order to measure a track for the backward proton. An updated setup around the target is illustrated in Fig. 4. In this setup, we made a simulation to identify the $\Sigma^0\pi^0$ decay mode. In Fig. 5 is plotted simulated missing mass of X obtained in the $d(K^-,n)p\pi^-X$

reaction, as a function of the produced hyperon mass (M_{Y^*}). Proton and pion are detected by BPC/BPD and CDC/CDH, respectively. Two decay modes of $\Sigma^0\pi^0$ and $\Lambda\pi^0$ assuming in an equal rate are plotted in the figure. Two loci corresponding to the $\Sigma^0\pi^0$ and $\Lambda\pi^0$ decay modes can be seen. Here, we define projection functions, F_{proj1} and F_{proj2}, along dashed and dash-dot lines. Distributions of the projection functions defined in Fig. 5 are shown in Figs. 6-a and 6-b. Two decay modes of $\Sigma^0\pi^0$ (blue) and $\Lambda\pi^0$ (red) are partly overlapped each other. We select the regions of F_{proj1} >0.01 and F_{proj2}>0.03 to estimate the efficiency and contamination of the $\Sigma^0\pi^0$ (blue) and $\Lambda\pi^0$ (red) decay modes, as demonstrated in Fig. 7.

We found that the detection efficiency of the $\Sigma^0\pi^0$ decay mode with employing the backward proton detector system much increases than that with only CDC/CDH. A two dimensional plot as of Fig. 5 is shown in Fig. 8. A projection function, F_{proj3}, is also defined along a dotted line in Fig. 8. In this case, distributions for the $\Sigma^0\pi^0$ (blue) and $\Lambda\pi^0$ (red) modes are much overlapped, as shown in Fig. 9-a. When we selected the region of F_{proj3} > -0.01, the detection efficiency and the contamination of the $\Sigma^0\pi^0$ (blue) and $\Lambda\pi^0$ (red) modes are obtained as a function of M_{Y^*} in Fig. 9-b. CDC/CDH is less effective for detection of the $\Sigma^0\pi^0$ decay.

In summary,

(1) The proposed experiment is aiming primarily to clarify whether Λ(1405) is a $\bar{K}N$ resonant state as predicted by the chiral unitary model or not. To accomplish the aim, we will measure the Λ(1405) state via the (K^-,n) reaction to test whether the resonance appears at ~1420 MeV/c^2 or ~1405 MeV/c^2.
(2) We re-confirmed that the (K^-,n) reaction is an ideal reaction to form the Λ(1405) state dominantly at a neutron forward angle.
(3) We expect to achieve the primary aim of measuring the position of the Λ(1405) state in the d(K^-,n) spectra in coincidences with $\Sigma^+\pi^-$ and $\Sigma^-\pi^+$ decay modes in high statistics. We expect to obtain the combined information of the *I=0* and *I=1* amplitudes as well as the cross (interference) terms between the two amplitudes in the d(K^-,n) reactions
(4) Contamination of the $\Sigma^*(1385)\rightarrow\Lambda\pi^0$ mode to the $\Lambda(1405)\rightarrow\Sigma\pi^0$ mode may be much reduced due to possible enhancement of Λ(1405) production by the d(K^-,n) reaction at a neutron forward angle. We will prepare to measure the Λ(1405) to $\Sigma^0\pi^0$ mode together with the $\Sigma^+\pi^-$ and $\Sigma^-\pi^+$ modes in order to obtain the decomposed information on the different isospin amplitudes in the d(K^-,n) reaction.

References:

[1] D. Jido, E. Oset, and T. Sekihara, “Kaonic production of Λ(1405) off deuteron target in chiral dynamics”, Eur.Phys.J.A42:257-268,2009.

[2] R. H. Dalitz and A. Deloff, J. Phys. G17, 289(1991).

[3] J. Yamagata-Sekihara、T. Sekihara, and D. Jido, paper in preparation; D. Jido, T. Sekihara, J. Yamagata-Sekihara, and H. Fujioka, private communication, Autumn, 2009.

[4] H. Fujioka et al., J-PARC Proposal P28, July 2009